JOC The Journal of Organic Chemistry

ARTICLE

pubs.acs.org/joc

Photolysis of (3-Methyl-2*H*-azirin-2-yl)-phenylmethanone: Direct Detection of a Triplet Vinylnitrene Intermediate

Sridhar Rajam,[†] Rajesh S. Murthy,[†] Abhijit V. Jadhav,[†] Qian Li,[†] Christopher Keller,[†] Claudio Carra,[§] Tamara C. S. Pace,[‡] Cornelia Bohne,[‡] Bruce S. Ault,[†] and Anna D. Gudmundsdottir*[,†]

[†]Department of Chemistry, University of Cincinnati, Ohio 45221-0172, United States

[‡]Department of Chemistry, University of Victoria, Victoria, BC, Canada

[§]Division of Space Life Science, Universities Space Research Association, Houston, Texas 77058, United States

Supporting Information

ABSTRACT: The photoreactivity of (3-methyl-2*H*-azirin-2-yl)-phenylmethanone, **1**, is wavelength-dependent (Singh et al. *J. Am. Chem. Soc.* **1972**, *94*, 1199−1206). Irradiation at short wavelengths yields **2P**, whereas longer wavelengths produce **3P**. Laser flash photolysis of **1** in acetonitrile using a 355 nm laser forms its triplet ketone (T_{1K}, broad absorption with $\lambda_{max} \sim$ 390−410 nm, $\tau \sim 90$ ns), which cleaves and yields triplet vinylnitrene **3** (broad absorption with $\lambda_{max} \sim$ 380−400 nm, $\tau = 2\ \mu$s). Calculations (B3LYP/6-31+G(d)) reveal that T_{1K} of **1** is located 67 kcal/mol above its ground state (S_0) and has a long C−N bond (1.58 Å), and the calculated transition state to form **3** is only 1 kcal/mol higher in energy than T_{1K} of **1**. The calculations show that **3** has significant 1,3-carbon iminyl biradical character, which explains why **3** reacts efficiently with oxygen and decays by intersystem crossing to the singlet surface. Photolysis of **1** in argon matrixes at 14 K produced ketene imine **7**, which presumably is formed from **3** intersystem crossing to **7**. In comparison, photolysis of **1** in methanol with a 266 nm laser produces mainly ylide **2** ($\lambda_{max} \sim$ 380 nm, $\tau \sim 6\ \mu$s, acetonitrile), which decays to form **2P**. Ylide **2** is formed via singlet reactivity of **1**, and calculations show that the first singlet excited state of the azirine chromophore (S_{1A}) is located 113 kcal/mol above its S_0 and that the singlet excited state of the ketone (S_{1K}) is 85 kcal/mol. Furthermore, the transition state for cleaving the C−C bond in **1** to form **2** is located 49 kcal/mol above the S_0 of **1**. Thus, we theorize that internal conversion of S_{1A} to a vibrationally hot S_0 of **1** forms **2**, whereas intersystem crossing from S_{1K} to T_{1K} results in **3**.

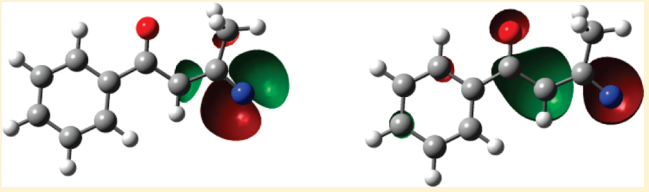

INTRODUCTION

Triplet nitrenes with electron-donating substituents, i.e., stabilized nitrenes such as alkyl and phenylnitrenes, are long-lived intermediates with lifetimes of milliseconds in solutions.[1−3] These triplet nitrenes are highly stabilized because they do not react with the solvent but rather decay by dimerization to form azo compounds.[1,2,4−6] For example, triplet phenylnitrenes have been stabilized in hemicarcerands and rendered stable in crystals.[7,8] In contrast, electron-deficient or less stable triplet nitrenes such as esternitrenes are more reactive and thus shorter-lived.[9,10] Calculations show that vinylnitrenes are stabilized just like phenyl- and alkylnitrenes.[11] The open shell singlet in vinylnitrene is 15 kcal/mol less stable than the triplet form and is thus comparable to the triplet−singlet gap of 18.5 kcal/mol for phenylnitrene.[12,13] Comparatively, the triplet−singlet gap in alkylnitrenes has been measured to be 38 kcal/mol.[14] Thus, the vinyl group reduces the singlet−triplet separation by approximately 20 kcal/mol as a result of the delocalization of the one unpaired electron and the corresponding reduction of electron−electron repulsions in the singlet state, which is similar to what has been observed for phenylnitrenes.

Although the calculation cited above supports the view that triplet vinylnitrene intermediates exist, there are no examples in the literature where such intermediates have been detected and characterized directly. Irradiation or thermal activation of simple vinyl azides yields azirine products, presumably via singlet vinylnitrene intermediates or in a concerted rearrangement from the excited state of the vinyl azide, rather than forming triplet vinylnitrenes.

There is evidence, however, that vinylnitrene intermediates are formed by photolyzing 2*H*-azirine derivatives.[15−21] For example, Singh and co-workers found that photolyzing **1** with light below 313 nm gives oxazole **2P**, whereas irradiation at 334 nm yields isoxazole **3P** (Scheme 1).[15] Singh et al. proposed that **2P** comes from cleaving the C−C bond in the azirine ring to form a singlet biradical **2**, whereas longer-wavelength irradiation was assumed to break the C−N bond in the azirine ring, yielding triplet vinylnitrene **3**.

Recent findings by Murata et al. further support that triplet vinylnitrenes are formed by photolyzing 2*H*-azirine because irradiating **4** at 366 nm at ambient temperature in the presence of oxygen and acrylonitrile yields 1-naphthaldehyde and **5** (Scheme 2).[21] These photoproducts can be attributed to trapping triplet

Received: April 29, 2011
Published: July 06, 2011

Scheme 1. Photoreactivity of 1 in Solution

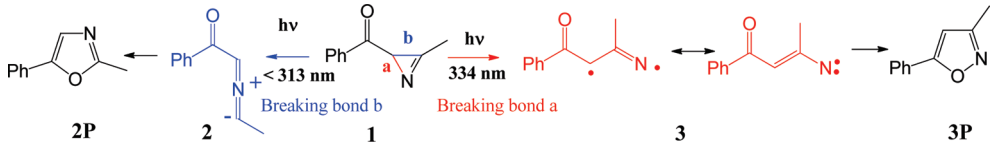

Scheme 2. Photolysis of 4

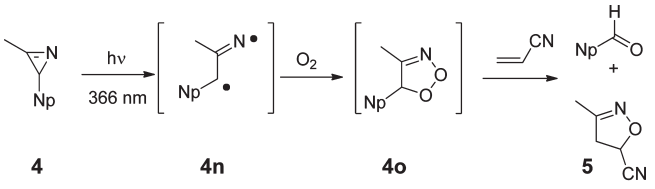

Np = Naphthalene

Scheme 3. Photolysis of 4 in Matrixes

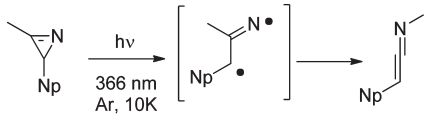

Scheme 4. Photolysis of 1 in Solution

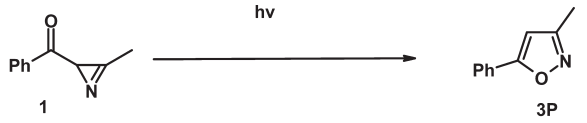

Reaction Conditions: a) >334 nm, Ar
b) >334 nm, O_2
c) >334 nm, O_2, CH_2CHCN

vinylnitrene **4n** with oxygen to form peroxide **4o**, which is presumably unstable and reacts further with acrylonitrile. Photolysis at 366 nm without trapping agents yielded no products because **4n** must undergo intersystem crossing and re-forms **4**. Furthermore, photolyzing **4** with 366 nm light in argon matrixes did not allow direct detection of **4n** because only the formation of ketene imine **6** was observed (Scheme 3). Murata and coworkers hypothesized that **4n** was formed in a vibrational excited state in the matrixes and rearranged into **6**.

In this paper we report the direct detection of triplet vinylnitrene **3** via the laser flash photolysis of **1**. Irradiation of **1** with a 355 nm laser resulted in the first excited triplet ketone (T_{1K}) of **1** ($\lambda_{max} \sim 390-410$ nm, τ = 90 ns, CH_3CN), which forms **3** ($\lambda_{max} \sim 380-400$ nm, $\tau = 2\,\mu$s, CH_3CN) selectively. In contrast, irradiation with a 266 nm laser results mainly in **2** ($\lambda_{max} \sim$ 380 nm, $\tau = 6\,\mu$s, CH_3CN). We used density functional theory (DFT) calculations to aid in the elucidation of the mechanism for forming **3**. The reactivity of **3** is unique and different from stabilized nitrenes such as triplet alkyl- and phenylnitrenes because **3** has a significant 1,3-carbon iminyl biradical character

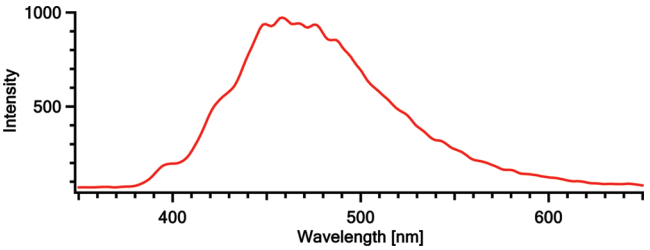

Figure 1. Phosphorescence spectrum of **1** in ethanol at 77 K.

and reacts more like a carbon centered radical rather than a nitrene intermediate.

RESULTS

Product Studies. Photolysis of **1** via a Pyrex filter yielded only **3P** (Scheme 4), whereas irradiation via a quartz filter gave **2P** (Scheme 1). This result is in agreement with product studies reported earlier by Singh et al.[15] Furthermore, irradiation of **1** via a Pyrex filter in an oxygen-saturated solution and the presence of acrylonitrile also yield **3P** as the only product, which demonstrates that one cannot trap any intermediates in solution with oxygen or acrylonitrile to yield any stable products.

Phosphorescence. The phosphorescence spectrum of **1** was obtained in ethanol glass at 77 K with excitation at 300 nm (Figure 1). The (0,0) band for the phosphorescence is estimated to be around 393 nm; thus the energy of the first excited triplet ketone (T_{1K}) of **1** is estimated to be 73 kcal/mol, which is 1−2 kcal lower than observed for acetophenone and propiophenone.[22]

Calculation. We calculated several stationary points on both the singlet and triplet potential energy surfaces of **1** (Figure 2) to better understand its photoreactivity and to aid in the characterization of the intermediates formed by irradiating **1**. The calculations further allowed us to clarify which excited states are the precursors to **2** and **3**, and this assignment was used to explain why the photochemistry of **1** is wavelength-dependent. All calculations were performed using Gaussian03 at a B3LYP level of theory using 6-31+G(d) as the basis set,[23−25] besides the calculated spectra in Tables 1, 2, and 3, which were calculated using MOLCAS6.

The ground state (S_0) geometry of **1** has C═O and C═N bonds with lengths of 1.23 and 1.25 Å, respectively, which are typical for carbonyl and iminyl moieties. Contrarily, the C−N bond in the azirine ring is 1.56 Å and is thus somewhat longer and weaker than a normal C−N bond, which is generally around 1.47 Å. Presumably, the electron-withdrawing effect of the carbonyl group weakens the C−N bond.

Time-dependent density functional theory (TD-DFT/B3LYP/6-31+G(d))[26−30] calculation on the optimized S_0 structure of **1** shows that its lowest energy electronic transitions are at

dx.doi.org/10.1021/jo200877k |J. Org. Chem. 2011, 76, 9934–9945

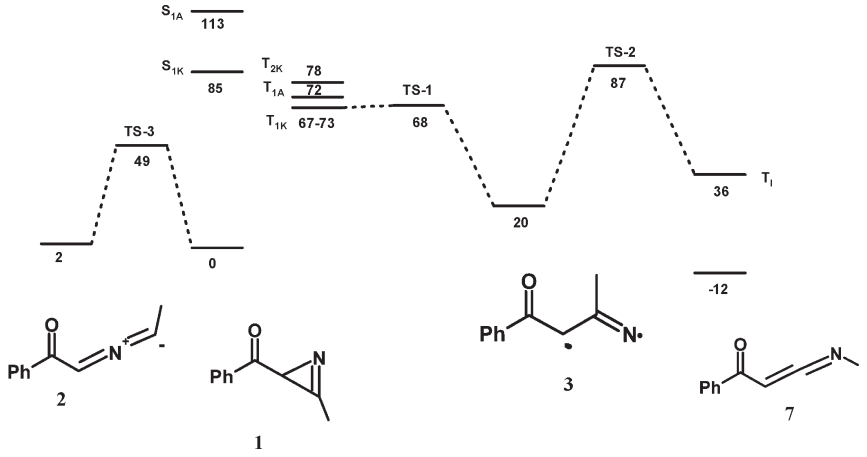

Figure 2. Stationary points on the triplet and singlet surfaces of **1**. The calculated energies are in kcal/mol. The energies for (a) **1**, **2**, **7** and TS-3 were obtained from B3LYP/6-31+G(d) calculations, (b) T_{1K} of **1** (67 kcal/mol), T_{1A} of **1**, TS-1, **3**, TS-2 and T_I of **7** were obtained from UB3LYP/6-31+G(d) calculations, (c) S_{1K} and S_{1A} of **1** were obtained from TD-DFT(B3LYP/6-31+G(d)) calculations on the S_0 geometry of **1** as obtained from B3LYP/6-31+G(d) calculation. (d) T_{1K} (73 kcal/mol) and T_{2K} of **1** were obtained from TD-DFT(UB3LYP/6-31+G(d)) calculations on the S_0 geometry of **1** as obtained from B3LYP/6-31+G(d) calculation.

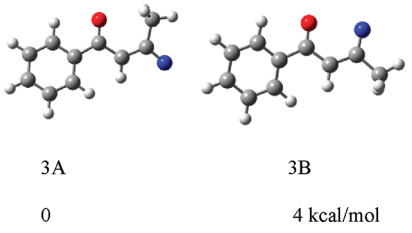

Figure 3. Relative energy of minimal energy conformers A and B of **3**.

Scheme 5. Bond Length and Spin Density As Obtained from B3LYP/6-31+G(d) Calculations of Triplet 3

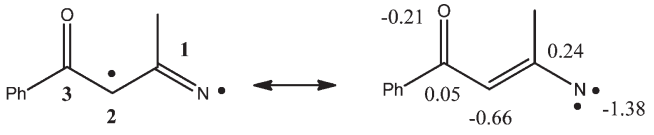

C(1)-N	1.30 Å
C(1)=C(2)	1.43 Å
C(2)-C(3)	1.46 Å
C(3)-Ph	1.50 Å
C(3)-O	1.24 Å

Calculated spin density
Explicitly spin state for **3**:
$S^2 = 2.046$
$S^2_A = 2.001$

338 nm (f = 0.0004) and 268 nm (f = 0.0149) and are due to electronic transitions out of the lone pair on the carbonyl group and the phenyl group into π^*-orbitals. In comparison, the bands at 252 nm (f = 0.3825) and 243 nm (f = 0.0267) are due to electronic transitions in the azirine and the arylketone moieties. Thus, irradiation of **1** at longer wavelengths selectively excited only the ketone moiety in **1**, whereas both the azirine and the arylketone absorb at lower wavelengths.

We used calculations to identify the various triplet excited states in **1** that are localized at different chromophores to identify the precursor to **3**. For example, TD-DFT (B3LYP/6-31+G(d)) calculations on the S_0 geometry of **1** located the first and the second excited state of the triplet ketone (T_{1K} and T_{2K}) in **1**, which were 73 and 78 kcal/mol above the S_0 of **1**. Analysis of the molecular orbitals indicates that the T_{1K} of **1** is mainly dominated by a (n,π^*) configuration, whereas T_{2K} has a (π,π^*) configuration. The energies of T_{1K} and T_{2K} in **1** are similar and consistent with the values measured for acetophenone.[31]

We also optimized T_{1K} of **1** using UB3LYP/6-31+G(d) and found that the C═N and the aromatic C═C bonds are not significantly changed in comparison to the S_0 of **1**. In contrast, the C═O bond is lengthened to 1.32 Å, which is consistent with the dominant (n,π^*) configuration of the T_{1K} of **1**.[32−34] Significantly, in the T_{1K} of **1**, the C−N bond length is 1.58 Å. This is slightly longer than the corresponding C−N bond in the S_0 of **1**, 1.56 Å, which indicates that the C−N bond is even weaker in the T_{1K} of **1**. The energy of the optimized T_{1K} of **1** is 67 kcal/mol above its S_0, which is notably lower than for the TD-DFT calculation. B3LYP optimizations, however, generally underestimate the energy of triplet ketones with a (n,π^*) configuration, whereas it estimated the energy of triplet ketones with (π,π^*) configuration more accurately.[35−37]

Similarly, we optimized the triplet excited state of the azirine chromophore (T_{1A}) in **1** and found that it is located 72 kcal/mol above the S_0 of **1**. The most significant difference between the S_0 and T_{1A} of **1** is that the C═N bond is longer in the T_{1A} of **1** (1.48 Å) than in the S_0 state (1.25 Å), which indicates that this bond is better described as a single bond. More importantly, however, the C−N bond in T_{1A} of **1** is only 1.48 Å, and thus the C−N bond in T_{1A} of **1** is significantly shorter than for the S_0 and T_{1K} states of **1**, 1.56 and 1.58 Å. Therefore, the calculations show that T_{1A} of **1** is not a likely precursor for **3**.

We found two minimal energy conformers for **3**, A and B, that are located 20 and 24 kcal/mol above the S_0 of **1** (Figure 3). The C−N and the C═C bond lengths of **3** are comparable to the values reported by Parasuk and Cramer for CH_2═CH—N: nitrene calculated by complete active space self consistent field (CASSCF) theory (Scheme 5).[11] We calculated the spin density for **3**, which suggests that **3** has significant 1,3-carbon iminyl biradical character, as the N atom has a spin density of only 1.38 and the C(2) atom of 0.66. The calculated rotational barrier between **3A** and **3B** is rather significant with a value of

dx.doi.org/10.1021/jo200877k |J. Org. Chem. 2011, 76, 9934–9945

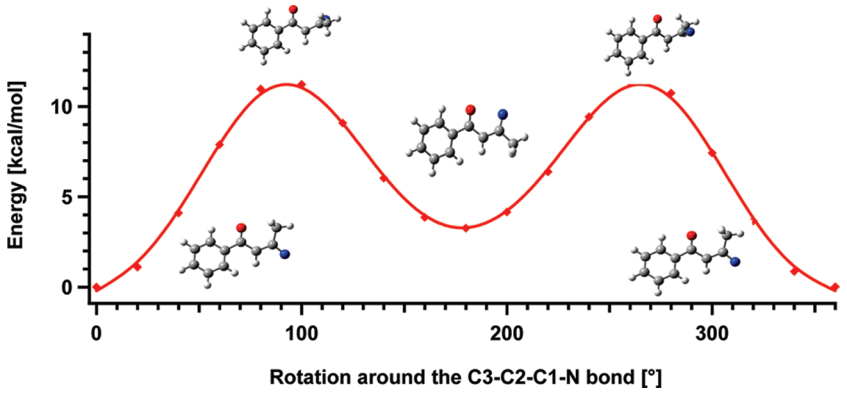

Figure 4. Calculated energy as a function of rotation around the C3−C2−C1−N bond in **3** (UB3LYP/6-31+G(d).

Scheme 6. Triplet Peroxide Radicals 8 and 9a, and Oxygen Ylides 9b and 9c

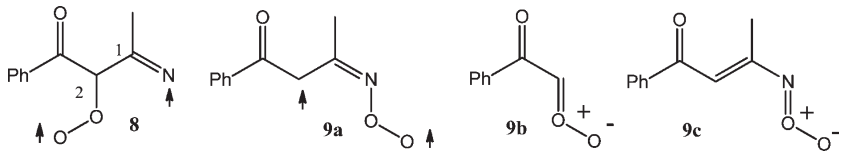

11 kcal/mol due to the conjugation between the vinylnitrene and carbonyl moieties (Figure 4).

The calculated triplet transition state (TS-1, Figure 2) for breaking the C−N bond in T_{1K} of **1** to form **3** is only 1 kcal/mol above the optimized structure of the T_{1K}. Intrinsic reaction coordinate[38−40] calculations correlate the T_{1K} of **1** and **3** to this transition state. Thus, formation of **3** is easily accessible from the T_{1K} of **1**, due to the weak C−N bond.

We also optimized the radical formed by trapping **3** with oxygen and found that **8** is 9 kcal/mol more stable than **3** and an oxygen molecule (Scheme 6). The addition of oxygen to **3** shortens the C−N bond length to 1.26 Å and lengthens the C1−C2 bond to 1.53 Å because the carbonyl and vinylnitrene groups are no longer in conjugation. The calculated triplet transition state for oxygen adding to **3** to form **8** is located 7 kcal/mol above **3** and an oxygen molecule. In comparison, addition of oxygen to the imine radical yields a peroxy radical (**9a**) that is 2 kcal/mol less stable than **3** and an oxygen molecule. The triplet transition state for forming **9a** is 15 kcal/mol above **3** and an oxygen molecule. Thus, the calculations show that trapping of **3** with an oxygen to form **8** can easily be done at ambient temperature and that the formation of **8** is strongly favored over **9a**. Optimization of **8** as a singlet results in **9b** and acetonitrile, which suggests that intersystem crossing of **8** to the singlet surface would yield these products. Similarly, optimization of **9a** as a singlet results in **9c**.

We optimized the structure of ketene imine **7**, which has C═C and C═N bonds that are 1.34 and 1.21 Å, respectively. The optimized triplet imine (T_I) of **7** is located 48 kcal/mol above the S_0 of **7**. The major difference between T_I and S_0 of **7** is that the C═C and C═N bonds (1.42 and 1.26 Å) are longer in the triplet state. The calculated triplet transition state for **3** to form T_I of **7** is located 67 kcal/mol above **3**. Thus, thermal rearrangement of **3** into **7** via T_I of **7** is not likely in solution. It is possible, however, that **3** can intersystem cross to form **7**.

We calculated the following points on the singlet potential surface of **1** to identify the excited state that results in **2**. TD-DFT calculations show that the first excited singlet ketone (S_{1K}) in **1** is 85 kcal/mol above S_0 and has an (n,π^*) configuration, whereas the first excited singlet state of the azirine moiety (S_{1A}) in **1** is 113 kcal/mol above S_0. The energy of S_{1A} in **1** obtained by TD-DFT fits well with what Bornemann and Klessinger have calculated for the energy for S_{1A} of 2*H*-azirine using CASSCF calculations.[41] The calculated singlet transition state for **2** forming **2P** is located 2 kcal/mol above **2**, which indicates that **2** can easily form **2P**.

The singlet transition state for breaking the C−C bond in **1** to form **2** was calculated to be 49 kcal/mol above the S_0 of **1**, and intrinsic reaction coordinates (IRC) calculations correlate this transition state with the S_0 of **1** and **2**. Thus, upon direct population of the S_{1A} of **1**, it can decay to a vibrationally hot ground state of **1** and form **2**. In comparison, the S_{1K} of **1** can be expected to intersystem cross to the triplet ketone with a similar rate constant as has been reported for acetophenone (10^{11} s^{-1}).[42−44]

The absorption spectra of T_{1K} **1**, **2**, and **3** were calculated by CASPT2 theory using atomic natural orbital (ANO-S) type basis sets contracted to single valence polarized basis sets (SVP). The CASSCF wave function was obtained using the state averaging technique, where all states were equally weighted. The active space includes the ten valence p orbitals adding either unpaired electrons or the lone pair of the nitrogen and oxygen.

Laser Flash Photolysis. The transient spectra obtained by laser flash photolysis of **1** with a 355 nm laser (15 ns)[45] gave a broad transient with λ_{max} between 390 and 410 nm for nitrogen purged solutions (Figure 5). The change in the transient spectra over time and the fact that the kinetics could not be fit to a mono-exponential function suggested that more than one transient was formed. The kinetics were adequately fit to the sum of two exponentials, taking into account a residual absorption, which

dx.doi.org/10.1021/jo200877k |*J. Org. Chem.* 2011, 76, 9934–9945

Table 1. Vertical Excitation Energies of the Triplet T_{1K} of ^{3}1, C_1 Symmetry[a]

state	ΔE_{CASSCF} eV	ΔE_{CASPT2} eV	ref weight[b]	λ nm	f[c]	major configurations[d]
T_1			0.69			61%: H-3 → L
T_2	0.27	0.48	0.69	2578	0.000160	53%: H → L
T_3	1.61	1.42	0.68	875	0.000003	31%: H-1 → L+1; 22%: H-5 → L
T_4	1.86	1.69	0.69	732	0.000270	20%: H → L+1; 34%: H-1 → L
T_5	2.22	1.84	0.68	673	0.000500	14%: H → L+3; 31%: H-1 → L+1; 19%: H-5 → L
T_6	2.67	2.26	0.67	548	0.000099	65%: H-4 → L+2
T_7	3.11	2.72	0.67	456	0.000003	30%: H-3 → L; 21%: H-3 → L+3
T_8	3.25	2.84	0.67	437	0.000032	21%: H-3 → L+1; 31%: H-1 → L+H-3 → L
T_9	3.53	2.95	0.68	420	0.000011	27%: H-3 → L+2; 30%: H-2 → L+2
T_{10}	3.89	3.22	0.66	384	0.000110	16%: H-5 → L+1

[a] Based on a CASPT2/CASSCF(14,13)/ANO-S wave function at the UB3LYP/6-31+G* geometry to eliminate the intruder states, with a level shift of 0.22 h applied to the CASPT2 wave function. [b] Weight of the zero order CASSCF in the CASPT2 wave function. [c] Oscillator strength for electronic transition. [d] Electron excitations within the active space.

Table 2. Vertical Excitation Energies of Triplet ^{3}3, C_1 Symmetry, Calculated by the CASPT2 Method[a]

state	ΔE_{CASSCF}, eV	ΔE_{CASPT2}, eV	ref weight[b]	λ, nm	f[c]	major configurations[d]
T_1			0.68			78%: H → L
T_2	2.29	1.69	0.68	734	2.2×10^{-4}	74%: H-3 → H
T_3	3.39	3.10	0.67	400	1.8×10^{-2}	30%: H-1 → L+1
						8%: H-2 → L+1
T_4	3.77	3.78	0.68	328	2.2×10^{-3}	46%: H-2 → L+1
						18%: [L → L+2, H-1 → H]
T_5	4.30	3.55	0.66	349	2.0×10^{-2}	14%: H-2 → H
						22%: [L → L+2, H-1 → H]
T_6	4.51	3.69	0.67	336	1.2×10^{-2}	30%: H-1 → H
						12%: H-1 → L+1
T_7	4.68	4.25	0.67	292	4.0×10^{-3}	25%: H-1 → L+1
						24%: H-2 → L+2

[a] Based on a CASPT2/CASSCF(14,13)/ANO-S wave function at the UB3LYP/6-31+G* geometry, to eliminate the intruder states, with a level shift of 0.2 h applied to the CASPT2 wave function. [b] Weight of the zero order CASSCF in the CASPT2 wave function. [c] Oscillator strength for electronic transition. [d] Electron excitations within the active space.

Table 3. Vertical Excitation Energies of Singlet ^{1}2, C_1 Symmetry, Calculated by the CASPT2 Method[a]

state	ΔE_{CASSCF}, eV	ΔE_{CASPT2}, eV	ref weight[b]	λ, nm	f[c]	major configurations[d]
S_0	0.00	0.00	0.69			77% of S_0
first	4.37	2.92	0.66	425	2.3×10^{-2}	60%: H-3 → L
second	4.67	3.30	0.66	376	5.6×10^{-1}	52%: H → L
third	4.74	3.91	0.68	317	4.4×10^{-2}	62%: H → L+3
fourth	4.79	3.77	0.64	329	9.9×10^{-2}	22%: H-2 → L
						18%: H-1 → L+3
fifth	5.97	4.67	0.63	266	1.3×10^{-1}	16%: H-1 → L + H → L
						13%: H-1 → L

[a] Based on a CASPT2/CASSCF(14,13)/ANO-S wave function at the B3LYP/6-31+G* geometry, to eliminate the intruder states, with a level shift of 0.2 h applied to the CASPT2 wave function. [b] Weight of the zero order CASSCF in the CASPT2 wave function. [c] Oscillator strength for electronic transition. [d] Electron excitations within the active space.

did not decay over the longest time scale studied (0.2 ms). The latter absorption presumably corresponds to the absorption of the product. The rate constants determined at 400 nm were 1.1×10^7 s^{-1} (τ = ~90 ns) and 3.7×10^5 s^{-1} (τ = ~3 μs) (Figure 6). For the reaction in methanol, the rate constants recovered were 4×10^6 s^{-1} (τ = ~250 ns) and 2×10^5 s^{-1} (τ = ~5 μs). Laser flash photolysis of **1** in oxygen-saturated acetonitrile showed the formation of transients with similar spectral features as observed under nitrogen (Figure 5B). However, the lifetimes of the transients were shorter under oxygen. The decay

dx.doi.org/10.1021/jo200877k |J. Org. Chem. 2011, 76, 9934–9945

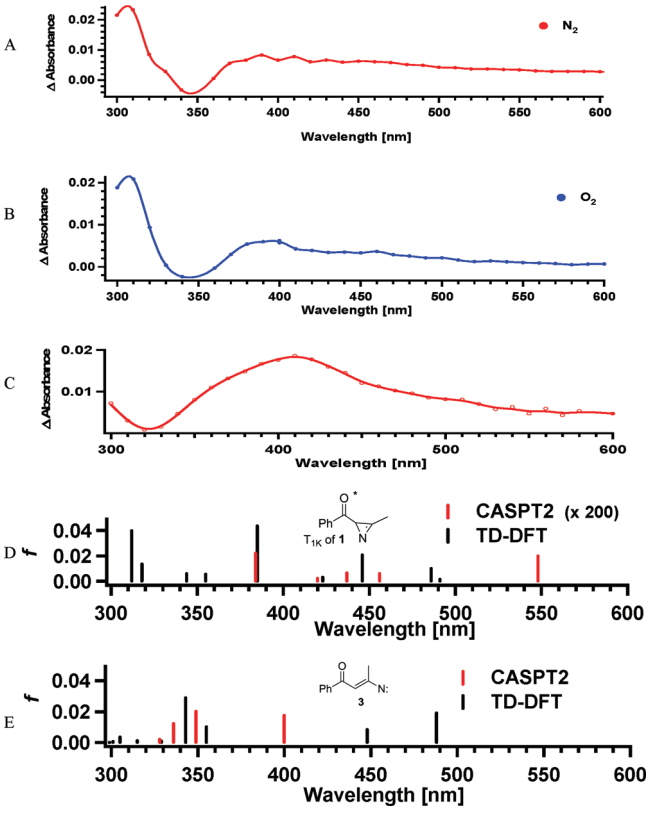

Figure 5. Laser flash photolysis of **1** with a 355 nm laser in (A) nitrogen-saturated acetonitrile collected between 19 and 110 ns after the laser pulse, (B) oxygen-saturated acetonitrile collected 19 and 110 ns after the laser pulse, and (C) nitrogen-saturated methanol collected between 0.12 and 0.70 μs after the laser pulse. (D) Calculated electronic transitions for T_{1K} of **1** using its UB3LYP/6-31+G(d) optimized geometry. The oscillators (f) for the CASPT2 transitions are multiplied by 200. (E) Calculated electronic transitions for **3** using its UB3LYP/6-31+G(d) optimized geometry.

could be fit to a monoexponential function and a residual constant absorption (Figure 6A). The rate constant for the decay was determined to be 1.5×10^7 s^{-1} (τ = ~67 ns). This value is similar to the short-lived component under nitrogen. The concentration of oxygen in acetonitrile is 0.02 M,[46] and a transient that reacts with a rate in excess of 3×10^9 M^{-1} s^{-1} would have a lifetime shorter than 17 ns and would not be detectable in the presence of oxygen. Therefore the kinetics under oxygen could be explained by two scenarios: (1) the short-lived transient under nitrogen is quenched with a rate close to diffusion control and the long-lived transient is also quenched by oxygen but with a lower rate (~7×10^8 M^{-1} s^{-1}), or (2) the short-lived transient does not react with oxygen and the long-lived transient is quenched with a rate close to diffusion control. Scenario (1), where both transients are quenched by oxygen, is the most likely one. The triplet states of acetophenones have been shown to have longer lifetimes in methanol because of a stabilization of the triplet with (π,π^*) configuration with respect to the reactive state with (n,π^*) configuration.[47] This solvent dependence was also observed for **1**, suggesting that the short-lived species under nitrogen is the T_{1K} of **1**, which is expected to be efficiently quenched by oxygen. In addition, phenyl- and alkylnitrenes were shown to react very slowly with oxygen, with rates between 10^4 and 10^7 M^{-1} s^{-1}.[1,48−50] Therefore, the assignment of the longer-lived transient under nitrogen to the nitrene is consistent with a quenching rate that is lower than for a diffusion-controlled process.

The assignment of the transient absorption to the T_{1K} of **1** and **3** was further supported with calculations. TD-DFT calculations of T_{1K} of **1** places the major electronic transitions at 312 nm (f = 0.0396), 385 nm (f = 0.0434), and 446 nm (f = 0.0205) (Figure 5D). In addition, there are less intense electronic transitions at longer wavelengths, 485 nm and 491 nm. The TD-DFT calculations place the major electronic transitions for **3** at 343 nm (f = 0.0288) and 488 nm (f = 0.0190) (Figure 5E). Thus, the TD-DFT calculations predict that T_{1K} of **1** will have maximum absorption at approximately 385 nm with the absorbance trailing out towards 500 nm and that **3** will have a broad absorption between ~340 and 490 nm. The overlapping TD-DFT spectra of T_{1K} of **1** and **3** fit well with the spectra in argon-saturated acetonitrile in Figure 5A that has λ_{max} between 390 and 410 nm. The band at 310 nm is exaggerated because of the absorption of the product **3P** (see the Supporting Information), which does not decay with time, nor is it quenched with oxygen. Furthermore, the transient spectrum obtained in argon-saturated methanol (Figure 5C) has a broad absorption with λ_{max} at 410 nm and a less intense product band at 310 nm, which also matches well with the overlapping TD-DFT spectra of T_{1K} of **1** and **3**.

Because the T_{1K} of **1** is quenched in oxygen-saturated acetonitrile, it is possible to obtain the transient absorption of **3** (Figure 5B) without the absorption of T_{1K} of **1**. The quenching of T_{1K} of **1** reduces the intensity of the transient absorption beside the band at 310 nm that is mainly due to product formation. The transient absorption of **3** has broad absorption with λ_{max} between 380 and 400 nm. The CASPT2 calculations place the major electronic transitions for **3** at 336 nm (f = 0.0123), 349 nm (f = 0.0210), and 400 nm (f = 0.0180) (Table 2), which match with observed λ_{max} for **3** being between 380 and 400 nm. In comparison, the TD-DFT calculation places the major absorption band for **3** at shorter wavelength or 343 nm, but the TD-DFT calculations predict more precisely that **3** will have broad absorption that trails out towards longer wavelengths.

The match between the CASPT2-calculated spectrum of T_{1K} of **1** (Table 1) and the experimental spectrum is disappointing. The CASPT2 calculations put the major bands for T_{1K} of **1** at 385 nm (f = 0.00011) and 548 nm (f = 0.000099) (Table 1). The band at 385 nm is in good agreement with the experimental spectra of T_{1K} of **1** and **3**, but the transient absorption around 548 nm is much less intense than the absorption between 380 and 410 nm. In addition, the CASPT2 calculated oscillators for T_{1K} of **1** are significantly weaker than the ones obtained from the TD-DFT calculations. However, it is complicated to compare oscillator strengths computed by different methods.[74,75]

In addition, TD-DFT calculations show that the absorption of the T_{1A} of **1** is somewhat similar to the absorption spectra of **3** (Supporting Information). However, the calculated potential energy surface shows that the T_{1K} of **1** is not likely to decay to form the T_{1A} of **1** because the latter state is higher in energy, and it would be expected to be quenched with oxygen with a rate close to that for diffusion.

Laser flash photolysis of **1** in nitrogen-saturated acetonitrile with a 266 nm laser (15 ns)[45] produced a transient spectrum with two absorption maxima at λ_{max} ~ 310 and 380 nm at short delays after the laser pulse (Figure 7). At long delays, a species with an

dx.doi.org/10.1021/jo200877k |J. Org. Chem. 2011, 76, 9934–9945

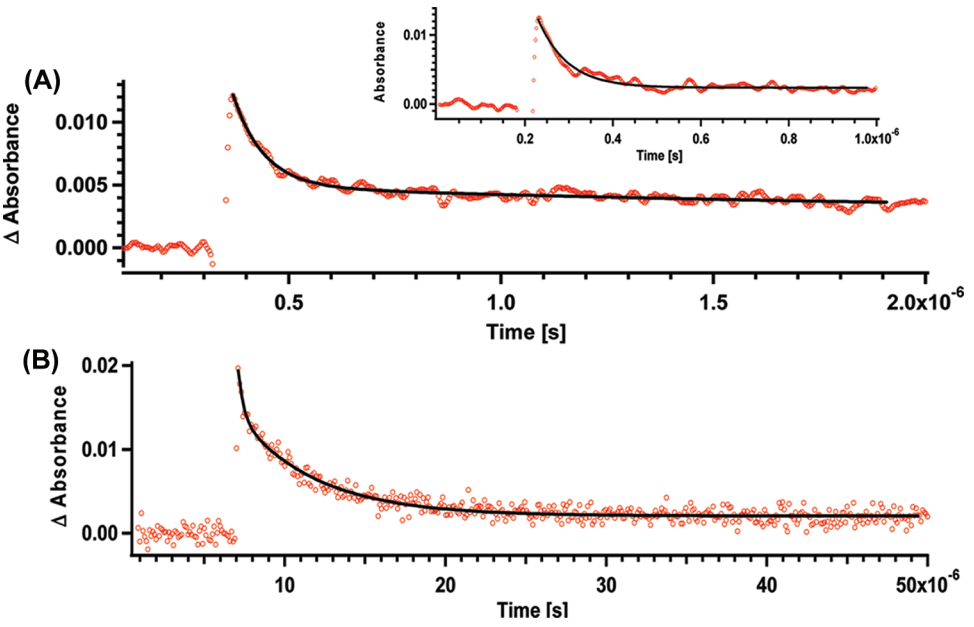

Figure 6. Kinetic traces monitored after irradiating **1** with a 355 nm laser (A) at 400 nm in N_2-saturated acetonitrile over a window of 2 μs and (B) at 410 nm in oxygen-saturated methanol over a window of 50 μs. (A) The black line corresponds to the fit to the sum of two exponentials with a finite final absorbance value. The inset shows the kinetics in O_2-saturated acetonitrile over a window of 1 μs. The black line corresponds to the fit to a monoexponential decay with a finite final absorbance value. (B) The black line corresponds to the fit to the sum of two exponentials with a finite final absorbance value.

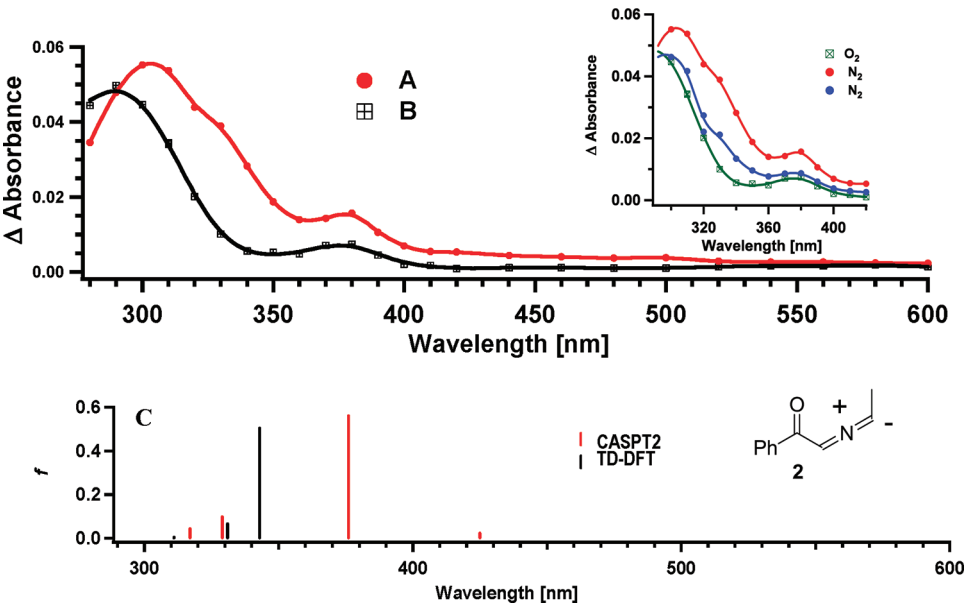

Figure 7. Laser flash photolysis of **1** with a 266 nm laser collected between (A) 0.19 and 1.3 μs (red trace) and between (B) 18 and 39 μs (black trace) after the laser pulse. The inset shows the transients of **1** with a 266 nm excitation in N_2-saturated acetonitrile collected between 0.19 and 1.3 μs (red trace) and between 1.6 and 5.3 μs (blue trace), and in O_2-saturated acetonitrile collected between 0.74 and 3.3 μs (green trace). (C) Calculated electronic transition for **2** using CASPT2 (gas phase) and TD-DFT (acetonitrile) calculations.

absorption maximum at 290 nm was observed. In comparison, in oxygen-saturated acetonitrile, laser flash photolysis of **1** produces a transient spectrum that has absorption maxima at $\lambda_{max} \sim 300$ and 380 nm. In oxygen-saturated solution, the absorption at 380 nm is formed faster than the resolution of the laser and it decays with a rate constant of 1.6×10^5 s^{-1} ($\tau \sim 6$ μs) (Figure 8), whereas at the 290 nm absorption, it does not decay over a time scale of 200 μs. The latter absorption was assigned to the absorption of the product. We assign the absorption band at 380 nm to **2** as validated by calculations. The calculated UV spectra of **2** using B3LYP TD-DFT in acetonitrile put the major electron transition in **2** at 343 nm ($f = 0.508$) and 331 nm ($f = 0.065$) due to promotion of electrons out of the C═N bond and the lone pair of the oxygen into the π^*-antibonding orbitals.

dx.doi.org/10.1021/jo200877k |J. Org. Chem. 2011, 76, 9934–9945

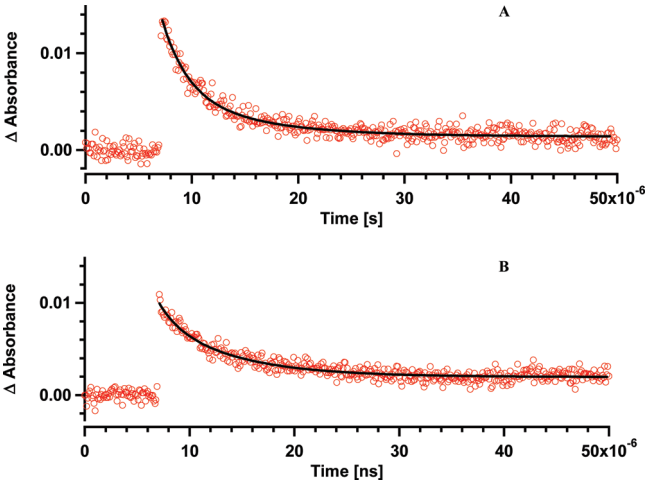

Figure 8. Kinetic traces monitored after irradiating with 266 nm laser over a window of 50 μs, (A) monitoring at 390 nm in N_2-saturated acetonitrile and (B) monitoring at 380 nm O_2-saturated acetonitrile.

Scheme 7. Ylides 5A, 5B, and 5C

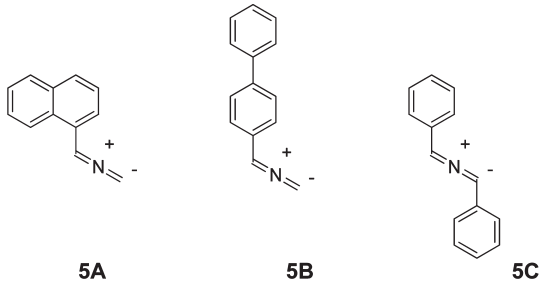

In comparison, the CASPT2 calculations place the major electron transition at 376 nm ($f = 0.56$), which corresponds to an excellent fit with the observed spectra. The absorption at 300 nm that does not decay significantly was assigned to the photoproduct.

In nitrogen-saturated acetonitrile, we observe a broadening of the transient spectrum at short delays, presumably due to the transient absorption of T_{1K} of **1** and of **3** in addition to **2** and the absorption of the photoproduct. The absorptions of the T_{1K} of **1** and of **3** were shown to be broad, and therefore identifying the individual transients was not possible. Thus, the decay at 390 nm in nitrogen-saturated acetonitrile can be fitted as a sum of two exponentials, with lifetimes of 6 and 2 μs, which can be attributed to **2** and **3**, respectively. It is important to note that the amplitude of the signals for T_{1K} of **1** and **3** are small because, with the excitation at 266 nm, the formation of **2** occurs concomitantly. In oxygen-saturated acetonitrile, a short-lived transient ($k = 1.5 \times 10^7$ s^{-1} or $\tau \sim 67$ ns) was observed, which is consistent with the shortening of the lifetime of **3** observed for the excitation of **1** with 355 nm.

Transient spectra of several ylides have been reported, and generally they are long-lived intermediates.[51−53] For example, **5A** has a lifetime of more than 100 μs, and **5B** has a lifetime of 13 ms (Scheme 7). It is reasonable, however, that **2** is shorter-lived than **5A** and **5B** because **2** undergoes an intramolecular reaction to form **2P**, whereas **5A** and **5B** decay by bimolecular

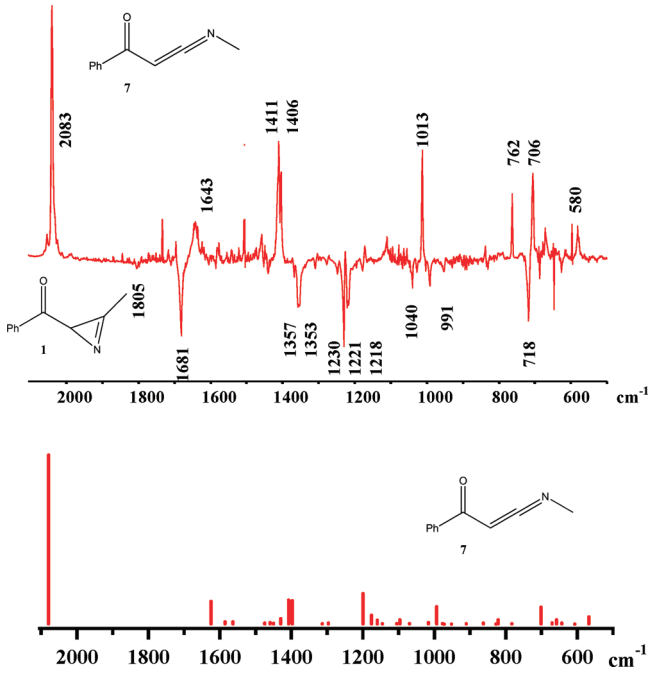

Figure 9. (A) Difference IR spectrum recorded after irradiation of **1** through a 340 nm filter. (B) Calculated IR spectrum for **7** (B3LYP/6-31+G(d)) scaled with 0.9613.

reactions. The λ_{max} for **5A**, **5B**, and **5C** was reported between 345 and 410 nm (Scheme 7), which is similar to the transient absorption of **2**.

Thus, the laser flash photolysis experiments for **1** showed that irradiation of **1** with 355 nm light produces the T_{1K} of **1**, which decays into **3**. Irradiation with 266 nm light results mainly in the formation of **2** and a smaller amount of T_{1K} of **1** and **3**.

Matrix Isolations. We deposited **1** into argon matrixes at 14 K. The carbonyl group in **1** has an intense band at 1681 cm^{-1}, and the imine band has a weak intensity at 1805 cm^{-1} (Figure 9). Irradiation of the matrix with a mercury arc lamp through a 340 nm filter caused the intensity of the bands at 1805, 1681, 1357, 1353, 1230, 1221, 1218, 1040, 1027, 991, and 718 cm^{-1} to be reduced. Simultaneously, a set of new bands were formed, and the most intense bands were located at 2083, 2080, 1643, 1411, 1406, 1013, 762, 706, and 580 cm^{-1}. We assign these new bands to ketene imine **7**, on the basis of its calculated IR spectra. The most intense peak in the IR spectra of **7** is the stretching of the cumulenic double bond C═C═N at 2083 cm^{-1}, which fits well with the calculated stretch at 2080 cm^{-1} after scaling by a factor of 0.9613.[54] The calculated stretch for the carbonyl group in **7** is located at 1625 cm^{-1} after scaling, which is also in a good agreement with the observed peak at 1643 cm^{-1}. In the calculated IR spectrum of ketene imine **7**, the bending of the C−H on the ketene imine and the bending in the methyl group are coupled and are located at 1407 and 1397 cm^{-1}, after scaling. We assign the vibrational bands at 1411 and 1406 cm^{-1} to these vibrational bending frequencies. The band at 1013 cm^{-1} is assigned to the bending of the C−H bond that is coupled with the stretching of the aromatic of the C═C bonds. These are calculated to be at 993 cm^{-1}, after scaling. Finally, we assign the vibration band at 580 cm^{-1} to the bending of the ketene imine band, which is calculated to be at 567 cm^{-1}, after scaling.

dx.doi.org/10.1021/jo200877k |*J. Org. Chem.* 2011, 76, 9934–9945

Irradiation of **1** in argon matrix with a Mineralight 254 nm UV lamp decreased the intensity of the same azirine vibrational bands as irradiation via a 340 nm filter. New IR bands at 2955, 2119, 1686, 1417, 1359, 1229, 963, 534, and 483 cm^{-1} were formed in addition to the IR bands assigned to **7** (Figure S5, Supporting Information). We assign these additional IR bands to **2**. The most intense bands at 2119 and 2098 cm^{-1} correlate to the cumulenic double bond C═N═C, which fits well with the calculated stretch of this band at 2074 cm^{-1} with scaling. The stretching of the C−H bonds in the methyl group was calculated to be at 2917 cm^{-1} with scaling, and this is in accordance with the experimentally observed band at 2955 cm^{-1}. The band at 1686 cm^{-1} is attributed to the carbonyl stretch on the basis of the calculated IR spectrum value of 1671 cm^{-1}. In the calculated IR spectrum of **2**, the bending of the C−H bond on the ylide carbon and the methyl group are coupled with vibrational frequencies at 1401 and 1360 cm^{-1}, with scaling. These are in good agreement with the experimentally observed bands at 1417 and 1359 cm^{-1}. The bending of the C−H bond on the ylide carbon coupled with the aromatic C−H bond is observed at 1229 cm^{-1}, which is a good fit with the calculated value of 1201 cm^{-1}, with scaling. The bending of the methyl group calculated at 993 cm^{-1} with scaling is assigned to the experimentally observed band at 963 cm^{-1}. Finally, the bending vibrations of the ylide group at 534 and 483 cm^{-1} are supported by the calculated IR values at 513 and 421 cm^{-1}, with scaling.

Thus, irradiation of **1** in matrixes via a 340 nm filter yields **7**, whereas broadband irradiation at ∼250 nm results in the formation of both **7** and **2** because the broad irradiation at lower wavelengths populates both S_{1A} and S_{1K} of **1**. S_{1A} of **1** reacts to form **2**, and the S_{1K} of **1** intersystem crosses to the triplet surface of **1**. We theorize that **3** can intersystem cross in matrixes to form **7** similar to how **3** can intersystem cross at room temperature to form **3P**. Presumably, in matrixes **3** intersystem crosses to reform **1**, which explains why **1** is not fully converted into **7** in the matrixes. However, restricted rotation prevents **3** from intersystem crossing to form **3P**.

DISCUSSION

The wavelength dependency of the photochemistry of **1** can be explained as follows: By irradiating above 300 nm, the ketone chromophore in **1** absorbs the light and forms the S_{1K} of **1**, which intersystem crosses to the T_{1K} of **1**. This results in the formation of **3**. The calculations demonstrate that the precursor to **3** is the T_{1K} of **1** rather than the T_{1A} of **1**. The electron withdrawing effect of the carbonyl group weakens the C−N bond in the T_{1K} of **1** and makes formation of **3** feasible. Thus, **3** is formed by the photoinitiated cleavage of the C−N bond in the T_{1K} of **1** rather than via triplet sensitization. Similarly, Fausto and co-workers have demonstrated that 2*H*-azirine derivatives with electron-withdrawing substituents are more prone to C−N bond cleavage of the azirine ring rather than the C−C bond cleavage.[16,17] In comparison, when irradiating with light below 300 nm, the azirine chromophore of **1** absorbs and forms S_{1A} of **1**, which undergoes internal conversion to form a vibrationally hot ground state that cleaves the C−C bond in the azirine chromophore to form **2**. However, irradiation with light below 300 nm also populates S_{1K} of **1** in competition with forming S_{1A} of **1**, which explains why the laser flash photolysis and the matrix isolation experiments showed formation of **7** and **3** as well as **2**.

Scheme 8. Possible Reactions of 3 with Oxygen

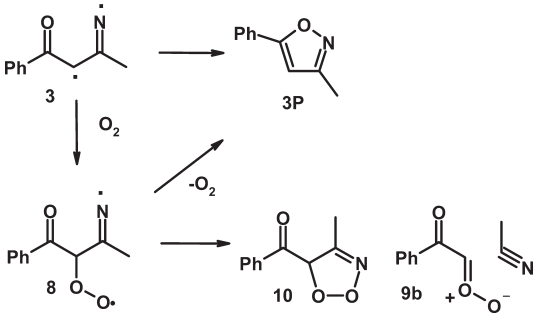

Laser flash photolysis allowed for the direct detection of **3** and shows that **3** has a broad absorption with λ_{max} at ∼380−400 nm. The transient absorption of **3** is shifted to longer wavelengths in comparison to the transient absorptions of triplet alkylnitrene (λ_{max} ∼ 320 nm)[1,35,55] and phenylnitrene (λ_{max} ∼ 310 nm).[56] The major electron transition in phenyl and alkylnitrenes is due to the promotion of an electron out of the lone pair of the nitrogen atom into the half-full orbital on the same nitrogen atom. In comparison, the major electronic transition in **3** involves transitions out of the lone pair on the oxygen and the CH═C—N: chromophore into the half full orbital on the nitrogen atom and the π^*-orbitals. Thus, the carbonyl and the vinyl chromophores in **3** are responsible for **3** having a broader absorption than triplet alkyl- and phenylnitrenes.

Vinylnitrene **3** decays by intersystem crossing to form **3P**, rather than dimerizing with another nitrene molecule as has been observed for stabilized triplet nitrenes, such as alkyl- and phenylnitrenes. Forming **3** in an oxygen-saturated solution does not lead to the formation of any new photoproduct that can be attributed to intercepting **3** with oxygen. Furthermore, forming **3** in an oxygen-saturated solution in the presence of acrylonitrile does not yield any new products. As described earlier, Inui and Murata also found that photolysis of **4** in oxygen-saturated solutions yielded no products.[21] However, they found that photolysis of **4** in the presence of oxygen and acrylonitrile produced **5** and 1-naphthaldehyde, and they proposed that oxygen traps vinylnitrene **4n** to form **4o**, which then reacts with acrylonitrile to form **5** and **6**. Laser flash photolysis of **1** show that **3** reacts with molecular oxygen with a rate of 7×10^8 M^{-1} s^{-1}, and thus we propose that **3** is trapped with oxygen to form **8**. Radical **8** does not, however, produce any new isolatable products (Scheme 8). The major difference between **3** and **4n** is that **3** has a carboxyl group that acts as an intramolecular trapping agent. It should be highlighted that the calculations show **8** is only 9 kcal/mol more stable than **3** and an oxygen molecule, and thus it is possible that the reaction is reversible. Generally, most simple aliphatic (sp^3) carbon radicals react exothermically (approximately −35 kcal/mol) with molecular oxygen, while the formation of peroxy radicals from vinyl and phenyl (sp^2) radicals are even more exothermic (approximately −45 kcal/mol).[57−60]

Triplet phenylnitrene derivatives and alkylnitrenes react with oxygen to form nitro products with much less efficiency than in **3**. The rates for phenylnitrene derivatives reacting with oxygen have been measured to be between 5×10^4 and 8×10^6 M^{-1} s^{-1}, and for alkylnitrene the rate is ∼5×10^4 M^{-1} s^{-1}.[1,48−50] The calculated activation barrier for triplet methylnitrene reacting with oxygen is considerably higher than for **3**, which explains why

dx.doi.org/10.1021/jo200877k |*J. Org. Chem.* 2011, 76, 9934–9945

Scheme 9. Calculated (B3LYP/6-31+G(d)) C−N Bond Length and Spin Density of Various Triplet Nitrenes

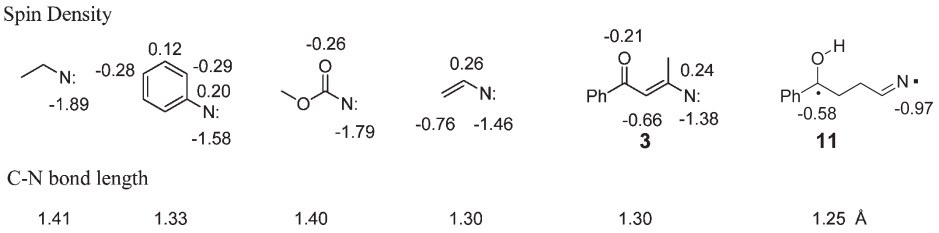

3 reacts faster with oxygen than do alkylnitrenes.[61] Since we did not observe formation of acetonitrile and **9b** or **10**, we conclude that **3** reacts with oxygen at a similar rate as observed for carbon centered radicals but does not yield stable products that we can isolate. However, it is also possible that the reaction is reversible.

We compared the optimized structure of **3** with the optimized structures of the simple triplet nitrenes shown in Scheme 9. The structures of these triplet nitrenes were also calculated using B3LYP/6-31+G(d) calculations.[62] The triplet ethyl- and esternitrenes have the longest C−N bonds of 1.40−1.41 Å, which indicates there is little interaction between the carbonyl groups and the nitrene moiety in the esternitrene. Similarly, the calculated spin density on the N atom in the triplet ethyl- and esternirenes is the largest because it is localized on the N-atom. In comparison, triplet phenylnitrene has a shorter C−N bond of 1.33 Å, which signifies some conjugation between the nitrogen atom and the phenyl moiety. This is further highlighted by the calculated spin density. The double bond character of the C−N bond and the delocalization of the spin density in CH_2═CH—N: and **3** demonstrate that these triplet nitrenes have significant 1,3-carbon iminyl biradical character, which explains why **3** reacts differently from the other triplet nitrenes in Scheme 9. Triplet vinylnitrene **3** does not dimerize as triplet alkyl- and phenylnitrenes, nor does it decay by hydrogen abstraction as the triplet esternitrene. Instead, it decays by intersystem crossing. Intersystem crossing in alkyl and phenylnitrene is a spin-forbidden process, which becomes allowed via spin−orbit and vibronic coupling.[63] Vibronic coupling, however, in triplet alkyl- and phenylnitrenes is expected to be small, because for monovalent nitrenes, only a few bending modes of the nitrene moiety are possible that modify the orbital structure to make state mixing possible. In contrast, vibronic coupling in **3** can be expected to be significant due to the conjugation of the vinylnitrene moiety with the carbonyl group and the 1,3-biradical character of **3**. Furthermore, we have previously shown that the 1,4 ketyl iminyl radical **11** also decays by intersystem crossing.[64]

Triplet vinylnitrenes have not been studied intensively because they are not formed by direct photolysis of azirines or vinyl azides. Generally, direct photolysis of simple azirines leads to formation of ylides rather than vinylnitrenes, unless the azirine has electron withdrawing substituents. Our studies show that triplet vinylnitrene **3** can be formed selectively, but it reacts differently from other stabilized triplet nitrenes, such as triplet phenyl- and alkylnitrenes which decay by dimerization. Even though **3** is more reactive than phenyl and alkylnitrenes, it does not react with the solvent as observed for electron deficient esternitrenes. Thus, triplet vinylnitrene **3** has unique reactivity, which is limited by intersystem crossing to form **3P**.

CONCLUSION

In conclusion, we have shown that the laser flash photolysis of **1** with 355 nm laser excitation results in formation of the T_{1K} of **1**, which cleaves to form **3**. The T_{1K} of **1** has a maximum absorption between 390 and 410 nm and a lifetime of ~90 ns in acetonitrile, whereas **3** has a broad absorption with λ_{max} between 380 and 400 nm and a lifetime of only a few microseconds. Vinylnitrene **3** decays via intersystem crossing to form **3P**. Furthermore, **3** reacts efficiently with oxygen, but oxygen trapping of **3** does not lead to any stable products. Thus, the reactivity of **3** highlights that it is best described as 1,3-carbon iminyl biradical rather than stabilized triplet nitrenes.

EXPERIMENTAL SECTION

Laser Flash Photolysis. Laser flash photolysis experiments were done with a neodymium-doped yttrium aluminum garnet (Nd:YAG) laser (355 and 266 nm, 15 ns).[45,64] Stock solutions of **1** in methanol or acetonitrile were prepared with spectroscopic grade solvents, such that the solutions had an absorption between 0.2 and 0.8 at 355 or 266 nm. Solutions were purged with nitrogen or oxygen for at least 15 min. Solutions of **1** are relatively photolabile and could be excited only with a small number of laser shots. For this reason, transient spectra were collected using a flow system, where a freshly prepared solution was pumped through a custom-designed Suprasil-cell (7 × 7 mm) at a rate of 1.5−2.0 mL/min. As a result, a fresh solution was irradiated by each laser shot. Decays were collected either by using the flow system or by subjecting the sample in static cells to a small number of laser shots and checking for the integrity of the sample with UV−vis spectroscopy. The kinetic traces were fitted so that the chi square value (the ratio of the curve fitting error to the standard deviation) is typically less than 0.02% of standard deviation of the measured data.

Calculations. All geometries were optimized at the B3LYP level of theory and with the 6-31G+(d) basis set as implemented in the Gaussian03 program.[24,25] All transition states were confirmed to have one imaginary vibrational frequency by analytical determination of the second derivatives of the energy, with respect to internal coordinates. Intrinsic reaction coordinate calculations were used to verify that the located transition states corresponded to the attributed reactant and product.[38,40] The absorption spectra were calculated using TD-DFT.[26−30]

Excitation energies and transition moments were computed by the CASPT2/CASSCF method[65,66] as implemented in the MOLCAS program,[67] using ANO-S type basis sets contracted to SVP basis set. The CASSCF wave functions were obtained using the state-averaging technique where all states were equally weighted. The active space has been defined as 13 MOs and 14 electrons, including the lone pair of the nitrogen atom. The CASPT2 values have been level-shifted by 0.2 h to avoid near degeneracy in the wave function. The effect of solvation was calculated using the self-consistent reaction field method with the integral equation formalism polarization continuum model with methanol as the solvent.[68−72]

Matrix Isolation. Matrix isolation studies were performed using conventional equipment.[73]

Photolysis of 1. *Photolysis of* ***1*** *in Argon-Saturated Acetonitrile.* A solution of **1** (6.29 mM, 1 mg/mL) in acetonitrile (dry) was placed into a Pyrex tube, and it was degassed by bubbling Ar for 20 min. The sample was irradiated with light from a 450 W high-pressure mercury lamp through a Pyrex filter (>310 nm) for 1 h. After irradiation, the solvent was evaporated under reduced pressure. ^{1}H NMR spectroscopy showed that a single photoproduct **3P** was formed in 80% yield, and the starting material **1** was recovered in 20% yield.

Photolysis of ***1*** *in Oxygen-Saturated Acetonitrile.* A solution of **1** (6.29 mM, 1 mg/mL) in acetonitrile (dry) was placed into a Pyrex tube, and O_2 was bubbled into the solution for 20 min. The sample was irradiated with light from a 450 W high-pressure mercury lamp through a Pyrex filter (>310 nm) for 1 h. After irradiation, the solvent was evaporated under reduced pressure. ^{1}H NMR spectroscopy showed that a single photoproduct **3P** was formed in 44% yield, and the starting material was recovered in 56% yield.

Irradiation of ***1*** *through Pyrex in Oxygen-Saturated Acetonitrile-*d_3. An oxygen-saturated solution of **1** in CH_3CN-d_3 with methyl benzoate as an internal standard was photolyzed through Pyrex. Analysis of the reaction mixture with ^{1}H NMR spectroscopy showed formation of **3P** and remaining **1**. However, integration of the ^{1}H NMR signals due to **1** and **3P** in comparison to the internal standard showed that the absolute chemical yields decreased with irradiation.

Irradiation of ***1*** *at Longer Wavelength.* A solution of **1** (6.29 mM, 1 mg/mL) and acrylonitrile (0.95 M) in acetonitrile (dry) was placed into a Pyrex tube, and O_2 was bubbled into the solution for 20 min. The sample was irradiated with light from a 450 W high-pressure mercury lamp through a light filter (>360 nm) for 1 h. After irradiation, the solvent was evaporated under reduced pressure. ^{1}H NMR spectroscopy showed that a single photoproduct **3P** was formed in 44% yield, and the starting material **3** was recovered in 56% yield.

■ ASSOCIATED CONTENT

Supporting Information. Cartesian coordinates, energies, and vibrational frequencies. This material is available free of charge via the Internet at http://pubs.acs.org.

■ AUTHOR INFORMATION

Corresponding Author

*E-mail: Anna.Gudmundsdottir@uc.edu.

■ ACKNOWLEDGMENT

We thank the National Science Foundation and the Ohio Supercomputer Center for supporting this work. S.R. thanks the UC Chemistry Department for a Twitchell fellowship. C.B. and T.C.S.P. thank the Natural Sciences and Engineering Council of Canada (NSERC) for support in the form of a discovery grant (C.B.) and a CGS-D fellowship (T.C.S.P.).

■ REFERENCES

(1) Singh, P. N. D.; Mandel, S. M.; Sankaranarayanan, J.; Muthukrishnan, S.; Chang, M.; Robinson, R. M.; Lahti, P. M.; Ault, B. S.; Gudmundsdottir, A. D. *J. Am. Chem. Soc.* **2007**, *129*, 16263.

(2) Li, Y. Z.; Kirby, J. P.; George, M. W.; Poliakoff, M.; Schuster, G. B. *J. Am. Chem. Soc.* **1988**, *110*, 8092.

(3) Platz M. S. In *Reactive Intermediate Chemistry*; Moss, R. A., Platz, M. S., Jones, M., Jr., Eds.; John Wiley & Sons: New York, 2004; pp 501−559.

(4) Sankaranarayanan, J.; Bort, L. N.; Mandel, S. M.; Chen, P.; Krause, J. A.; Brooks, E. E.; Tsang, P.; Gudmundsdottir, A. D. *Org. Lett.* **2008**, *10*, 937.

(5) Leyva, E.; Platz, M. S.; Persy, G.; Wirz, J. *J. Am. Chem. Soc.* **1986**, *108*, 3783.

(6) Klima, R. F.; Gudmundsdottir, A. D. *J. Photochem. Photobiol., A* **2004**, *162*, 239.

(7) Mahe, L.; Izuoka, A.; Sugawara, T. *J. Am. Chem. Soc.* **1992**, *114*, 7904.

(8) Warmuth, R.; Makowiec, S. *J. Am. Chem. Soc.* **2007**, *129*, 1233.

(9) Buron, C.; Platz, M. S. *Org. Lett.* **2003**, *5*, 3383.

(10) Murthy, R. S.; Muthukrishnan, S.; Rajam, S.; Mandel, S. M.; Ault, B. S.; Gudmundsdottir, A. D. *J. Photochem. Photobiol., A* **2009**, *201*, 157.

(11) Parasuk, V.; Cramer, C. J. *Chem. Phys. Lett.* **1996**, *260*, 7.

(12) McDonald, R. N.; Davidson, S. J. *J. Am. Chem. Soc.* **1993**, *115*, 10857.

(13) Travers, M. J.; Cowles, D. C.; Clifford, E. P.; Ellison, G. B. *J. Am. Chem. Soc.* **1992**, *114*, 8699.

(14) Travers, M. J.; Cowles, D. C.; Clifford, E. P.; Ellison, G. B.; Engelking, P. C. *J. Chem. Phys.* **1999**, *111*, 5349.

(15) Singh, B.; Zweig, A.; Gallivan, J. B. *J. Am. Chem. Soc.* **1972**, *94*, 1199.

(16) Kaczor, A.; Gomez-Zavaglia, A.; Cardoso, A. L.; Melo, T. M. V. D. P.; Fausto, R. *J. Phys. Chem. A* **2006**, *110*, 10742.

(17) Gomez-Zavaglia, A.; Kaczor, A.; Coelho, D.; Cristiano, M. L. S.; Fausto, R. *J. Mol. Struct.* **2009**, *919*, 271.

(18) Inui, H.; Murata, S. *Chem. Lett.* **2001**, 832.

(19) Inui, H.; Murata, S. *Chem. Commun. (Cambridge, U. K.)* **2001**, 1036.

(20) Inui, H.; Murata, S. *Chem. Phys. Lett.* **2002**, *359*, 267.

(21) Inui, H.; Murata, S. *J. Am. Chem. Soc.* **2005**, *127*, 2628.

(22) Murov, S. L.; Carmichael, I.; Hug, G. L. *Handbook of Photochemistry*, 2nd ed.; Marcel Dekker, Inc.: New York, 1993.

(23) Frisch, M. J.; Trucks, G. W.; Schlegel, H. B.; Scuseria, G. E.; Robb, M. A.; Cheeseman, J. R.; Montgomery, J. A., Jr.; Vreven, T.; Kudin, K. N.; Burant, J. C.; Millam, J. M.; Iyengar, S. S.; Tomasi, J.; Barone, V.; Mennucci, B.; Cossi, M.; Scalmani, G.; Rega, N.; Petersson, G. A.; Nakatsuji, H.; Hada, M.; Ehara, M.; Toyota, K.; Fukuda, R.; Hasegawa, J.; Ishida, M.; Nakajima, T.; Honda, Y.; Kitao, O.; Nakai, H.; Klene, M.; Li, X.; Knox, J. E.; Hratchian, H. P.; Cross, J. B.; Bakken, V.; Adamo, C.; Jaramillo, J.; Gomperts, R.; Stratmann, R. E.; Yazyev, O.; Austin, A. J.; Cammi, R.; Pomelli, C.; Ochterski, J. W.; Ayala, P. Y.; Morokuma, K.; Voth, G. A.; Salvador, P.; Dannenberg, J. J.; Zakrzewski, V. G.; Dapprich, S.; Daniels, A. D.; Strain, M. C.; Farkas, O.; Malick, D. K.; Rabuck, A. D.; Raghavachari, K.; Foresman, J. B.; Ortiz, J. V.; Cui, Q.; Baboul, A. G.; Clifford, S.; Cioslowski, J.; Stefanov, B. B.; Liu, G.; Liashenko, A.; Piskorz, P.; Komaromi, I.; Martin, R. L.; Fox, D. J.; Keith, T.; Al-Laham, M. A.; Peng, C. Y.; Nanayakkara, A.; Challacombe, M.; Gill, P. M. W.; Johnson, B.; Chen, W.; Wong, M. W.; Gonzalez, C.; Pople, J. A. *Gaussian 03*, Revision A.1; Gaussian, Inc.: Wallingford, CT, 2004.

(24) Becke, A. D. *J. Chem. Phys.* **1993**, *98*, 5648.

(25) Lee, C.; Yang, W.; Parr, R. G. *Phys. Rev. B: Condens. Matter* **1988**, *37*, 785.

(26) *Density Functional Methods in Chemistry*; Labanowksi, J. K.; Andzelm, J. W., Eds.; Springer-Verlag: New York, 1991.

(27) Parr, R. G.; Weitao, Y. *Density Functional Theory in Atoms and Molecules*; Oxford University Press: Oxford, 1989.

(28) Stratmann, R. E.; Scuseria, G. E.; Frisch, M. J. *J. Chem. Phys.* **1998**, *109*, 8218.

(29) Foresman, J. B.; Head-Gordon, M.; Pople, J. A.; Frisch, M. J. *J. Phys. Chem.* **1992**, *96*, 135.

(30) Bauernschmitt, R.; Ahlrichs, R. *Chem. Phys. Lett.* **1996**, *256*, 454.

(31) Ghoshal, S. K.; Sarkar, S. K.; Kastha, G. S. *Bull. Chem. Soc. Jpn.* **1981**, *54*, 3556.

(32) Srivastava, S.; Yourd, E.; Toscano, J. P. *J. Am. Chem. Soc.* **1998**, *120*, 6173.
(33) He, H.-Y.; Fang, W.-H.; Phillips, D. L. *J. Phys. Chem. A* **2004**, *108*, 5386.
(34) Fang, W.-H.; Phillips, D. L. *J. Theor. Comput. Chem.* **2003**, *2*, 23.
(35) Muthukrishnan, S.; Mandel, S. M.; Hackett, J. C.; Singh, P. N. D.; Hadad, C. M.; Krause, J. A.; Gudmundsdottir, A. D. *J. Org. Chem.* **2007**, *72*, 2757.
(36) Muthukrishnan, S.; Sankaranarayanan, J.; Pace, T. C. S.; Konosonoks, A.; De, M. M. E.; Meese, M. J.; Bohne, C.; Gudmundsdottir, A. D. *J. Org. Chem.* **2010**, *75*, 1393.
(37) Ranaweera, R. A. A. U.; Zhao, Y.; Muthukrishnan, S.; Keller, C.; Gudmundsdottir, A. D. *Aust. J. Chem.* **2010**, *63*, 1645.
(38) Gonzalez, C.; Schlegel, H. B. *J. Chem. Phys.* **1989**, *90*, 2154.
(39) Fukui, K. *Acc. Chem. Res.* **1981**, *14*, 363.
(40) Gonzalez, C.; Schlegel, H. B. *J. Phys. Chem.* **1990**, *94*, 5523.
(41) Bornemann, C.; Klessinger, M. *Chem. Phys.* **2000**, *259*, 263.
(42) Borkman, R. F.; Kearns, D. R. *Chem. Commun. (London)* **1966**, 446.
(43) Lamola, A. A.; Hammond, G. S. *J. Chem. Phys.* **1965**, *43*, 2129.
(44) McGarry, P. F.; Doubleday, C. E., Jr.; Wu, C.-H.; Staab, H. A.; Turro, N. J. *J. Photochem. Photobiol., A* **1994**, *77*, 109.
(45) Liao, Y.; Bohne, C. *J. Phys. Chem.* **1996**, *100*, 734.
(46) Clark, W. D. K.; Steel, C. *J. Am. Chem. Soc.* **1971**, *93*, 6347.
(47) Wagner, P. J.; Truman, R. J.; Scaiano, J. C. *J. Am. Chem. Soc.* **1985**, *107*, 7093.
(48) Liang, T. Y.; Schuster, G. B. *J. Am. Chem. Soc.* **1987**, *109*, 7803.
(49) Pritchina, E. A.; Gritsan, N. P. *J. Photochem. Photobiol., A* **1988**, *43*, 165.
(50) Gritsan, N. P.; Pritchina, E. S. *J. Inf. Rec. Mater.* **1989**, *17*, 391.
(51) Barcus, R. L.; Wright, B. B.; Platz, M. S.; Scaiano, J. C. *Tetrahedron Lett.* **1983**, *24*, 3955.
(52) Naito, I.; Morihara, H.; Ishida, A.; Takamuku, S.; Isomura, K.; Taniguchi, H. *Bull. Chem. Soc. Jpn.* **1991**, *64*, 2757.
(53) Naito, I.; Morihara, H.; Ishida, A.; Takamuku, S.; Isomura, K.; Taniguchi, H. *Bull. Chem. Soc. Jpn.* **1991**, *64*, 2757.
(54) Foresman, J. B.; Frisch, Æ. *Exploring Chemistry with Electronic Structure Methods*, 2nd ed.; Gaussian, Inc.: Pittsburgh, PA, 1996; p 64.
(55) Singh, P. N. D.; Mandel, S. M.; Robinson, R. M.; Zhu, Z.; Franz, R.; Ault, B. S.; Gudmundsdottir, A. D. *J. Org. Chem.* **2003**, *68*, 7951.
(56) Gritsan, N. P.; Zhu, Z.; Hadad, C. M.; Platz, M. S. *J. Am. Chem. Soc.* **1999**, *121*, 1202.
(57) Marchaj, A.; Kelley, D. G.; Bakac, A.; Espenson, J. H. *J. Phys. Chem.* **1991**, *95*, 4440.
(58) Eskola, A. J.; Timonen, R. S. *Phys. Chem. Chem. Phys.* **2003**, *5*, 2557.
(59) Sommeling, P. M.; Mulder, P.; Louw, R.; Avila, D. V.; Lusztyk, J.; Ingold, K. U. *J. Phys. Chem.* **1993**, *97*, 8361.
(60) Fahr, A.; Laufer, A. H. *J. Phys. Chem.* **1988**, *92*, 7229.
(61) Liu, J.; Hadad, C. M.; Platz, M. S. *Org. Lett.* **2005**, *7*, 549.
(62) Sankaranarayanan, J.; Rajam, S.; Hadad, C. M.; Gudmundsdottir, A. D. *J. Phys. Org. Chem.* **2010**, *23*, 370.
(63) Salem, L.; Rowland, C. *Angew. Chem., Int. Ed. Engl.* **1972**, *11*, 92.
(64) Muthukrishnan, S.; Sankaranarayanan, J.; Klima, R. F.; Pace, T. C. S.; Bohne, C.; Gudmundsdottir, A. D. *Org. Lett.* **2009**, *11*, 2345.
(65) Roos, B. O. *Ab Initio Methods in Quantum Chemistry, Part 2*; Wiley: Chichester, UK, 1987; Vol. 69.
(66) Andersson, K.; Malmqvist, P. A.; Roos, B. O.; Sadlej, A. J.; Wolinski, K. *J. Phys. Chem.* **1990**, *94*, 5483.
(67) *MOLCAS*, Version 6.0. Karlström, G.; Lindh, R.; Malmqvist, P.-Å.; Roos, B. O.; Ryde, U.; Veryazov, V.; Widmark, P.-O.; Cossi, M.; Schimmelpfennig, B.; Neogrady, P.; Seijo, L. *Comput. Mater. Sci.* **2003**, *28*, 222.
(68) Tomasi, J.; Mennucci, B.; Cammi, R. *Chem. Rev.* **2005**, *105*, 2999.
(69) Mennucci, B.; Cances, E.; Tomasi, J. *J. Phys. Chem. B* **1997**, *101*, 10506.
(70) Cances, E.; Mennucci, B. *J. Chem. Phys.* **2001**, *114*, 4744.
(71) Tomasi, J.; Persico, M. *Chem. Rev. (Washington, DC)* **1994**, *94*, 2027.
(72) Cramer, C. J.; Truhlar, D. G. *Chem. Rev. (Washington, DC)* **1999**, *99*, 2161.
(73) Ault, B. S. *J. Am. Chem. Soc.* **1978**, *100*, 2426.
(74) Caricato, M.; Trucks, G. W.; Frisch, M. J.; Wiberg, K. B. *J. Chem. Theory Comput.* **2011**, *7*, 456.
(75) Ljubic, I.; Sabljic, A. S. *J. Phys. Chem. A* **2011**, *115*, 4840.